Progress In Electromagnetics Research M, Vol. 50, 95–104, 2016

A Comparison among Different Kinds of Stator Lamination in Tubular Linear Machines

Giovanni Cipriani[1], Mattia Corpora[1], Vincenzo Di Dio[1, *], Antonio Musolino[2], Rocco Rizzo[2], and Luca Sani[2]

Abstract—In this paper the authors perform a comparison among three different stator structures for a Tubular Permanent Magnet Linear Machine. Each structure is characterized by its own lamination which is expected to contribute to the overall performance of the machine. A detailed analysis of the main figures of merit of the three configurations has been carried out in order to identify the configuration with the best characteristics. Significant data such as flux distribution, rated voltage and current, force on the moved and power losses have been compared. The results show that the choice of a mixed stator lamination allows to improve the performance of these machines.

1. INTRODUCTION

In recent years, scientific interest for the study of linear machines has grown significantly due to different characteristics that make them particularly appropriate for different applications [1–3]. These applications include, for example, transport, automation, materials processing, medical care and energy generation systems [4]. In particular, the use of tubular linear generator as a wave energy converter in marine environment presents a number of advantages. The tubular geometry of this kind of machines presents a mechanical isotropy in the transverse direction, allowing a natural reaction to the off-centering actions due to the marine currents. Moreover, because of its almost closed structure, this machine can be easily protected against the corrosion of the marine environment.

The substantial advantage of the use of linear machines, where it is necessary to obtain a translational motion, is the absence of a transmission system that is indispensable in rotating machines. This advantage allows to increase their performance, robustness and reliability. Among various types of linear machines, tubular permanent magnet machines (TPMLMs) have interesting features such as high force density, high efficiency, zero attraction force between the movable and fixed part and excellent dynamic characteristics [5]. Depending on the path followed by the magnetic flux lines, the TPMLMs are divided in longitudinal flow machines (LFTPMLM) and in transverse flux machines (TFTPMLM). In both types of machines, it is essential to have a stator structure that is able to provide optimal closed paths for the magnetic field flux lines and at the same time to limit the loss phenomena. As in rotating machines, the strategy used to limit iron losses is lamination. However, this strategy significantly influences the machine performance. In fact, although the lamination contributes to reduce the eddy currents in the ferromagnetic core and therefore to improve the overall machine efficiency, it also may increase the magnetic reluctance. This latter fact results in a reduction of the useful flux with a consequent performance decrease in both the operation of the machine as a generator and as a motor. In this work, some characteristics of three different types of three-phase machines with short stator and long translator will be analyzed. The translator, which is the same for all the stator types, is composed

Received 12 July 2016, Accepted 4 September 2016, Scheduled 20 September 2016

* Corresponding author: Vincenzo Di Dio (vincenzo.didio@unipa.it).

[1] DEIM, Department of Energy, Engineering Information and Mathematical Model, University of Palermo, Palermo, Italy. [2] DESTEC, Department of Energy and Systems Engineering, University of Pisa, Italy.

of ferrite ring magnets and iron rings in almost Halbach configuration. In particular, it is built by stacking four ferrite rings, magnetized in the axial direction, and an iron ring (see Figure 6). The stator windings structure, that is common to all the machines here considered, consists of coils connected together in such a way as to obtain a three-phase, Y-connected, 4-pole machine. The considered stator windings current density allows all the machines to develop a rated power of 1 kW, if a corresponding mechanical input is applied. The three machines, object of this study, will differ for the magnetic core type. In particular, three different structures both in geometric terms and in lamination strategy terms are compared. Two of which are known in the literature, while the third one is an innovative structure, proposed by the authors. Then, by using a 3D FEM code, these three structures are investigated in order to identify the solution which presents the best characteristics in terms of performance. The analysis is carried out by comparing the significant data as flux, voltages, currents, forces and iron losses.

2. ANALYZED TPMLM STRUCTURES

2.1. Stator Structures

Figure 1 shows the first stator structure. The stator iron core is built by packing laminations of a thickness of 0.5 mm having the form of a disk with two different inner radii and equal outer radii and in such a way as to create the stator slots on which windings are located. In this structure, the lamination direction is parallel to the translation axis of the movable part of the machine. In teeth, where the field lines have a radial direction (i.e., where crossing the air gap), this type of lamination allows to confine the eddy currents in the single sheet volume. On the contrary, this does not occur when the flux has axial direction as in the stator back iron. Moreover, this structure introduces additional air gaps in the path of the axial direction of the field, determining a substantial performance decrease. It should also be specified that this type of structure has two interesting features: the first one is that the translator being completely surrounded by the stator allows to obtain a better usage of the iron; in addition, this structure is constructively simple, robust and has reduced manufacturing costs.

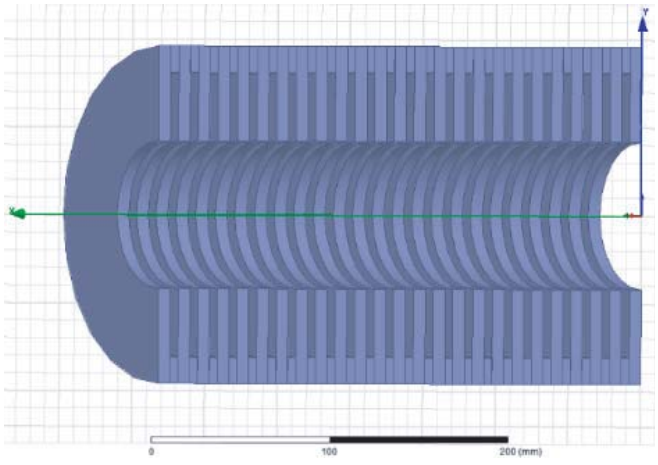

Figure 1. First stator structure.

The second stator version of the machine provides for the assembly of 8 blocks, whose lamination direction is perpendicular to the motion direction (see Figure 2). The choice of the number of sectors is dictated by constructive practicality issues. The larger the circumference is, the greater the number of sectors is, since the thickness of each sector cannot be too small for mechanical resistance issues. It is also true that the choice of sectors too thick in relation to the circumference of the air gap affects the radial distribution of the magnetic flux due to the adopted lamination.

In this second structure, the blocks are made up of combs to realize the stator slots. Furthermore, the sheets are positioned in such a way as to envelop the profile of a cylinder to accommodate the

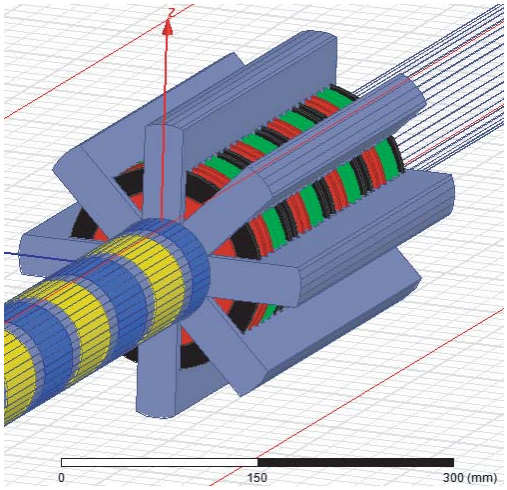

Figure 2. Second stator structure.

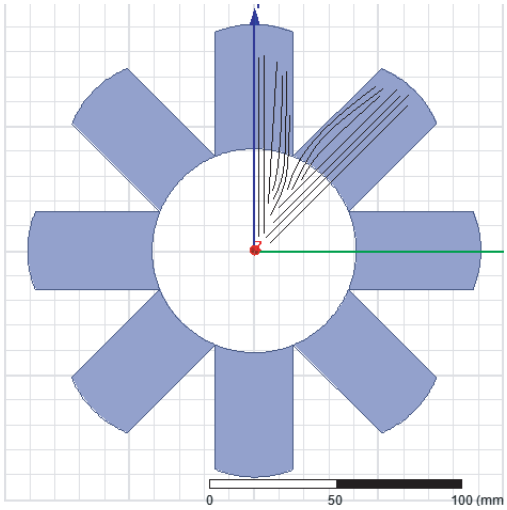

Figure 3. Second structure: magnetic field lines in the border areas.

translator. This configuration has the interesting feature to confine the eddy currents within the sheet both for the lines of field in the axial direction and in radial direction. Moreover, this structure does not introduce, as the previous one, further air gaps. However, for this configuration it is necessary to make some considerations. In fact this type of structure could lead the peripheral areas of the blocks close to the translator saturation (because the useful volume was reduced since the translator is no longer surrounded by a cylinder made of iron but by a finite inter-spaced number of blocks). In other words, unlike the first configuration, the volume of ferromagnetic material is not distributed homogeneously around the translator but prefers only the areas in which there are the blocks by increasing the field intensity in the areas of junction between a block and the adjacent one (see Figure 3). Also not to be overlooked are the construction problems that introduce the necessary and complex mechanical devices designed to align the sheets accurately along the axis of the machine and to give strength and structure to the stator.

The third (innovative) configuration (see Figure 4) is a combination of the two previous structures. It is able to integrate the advantageous characteristics of the two previously presented types. In particular, this structure involves the construction of laminated disks with a vector of rolling parallel to the axis of motion (as for the first structure) of which the outer radius, however, has a size such as to ensure only the depth of the slots. On this cylinder are placed the blocks with vector lamination

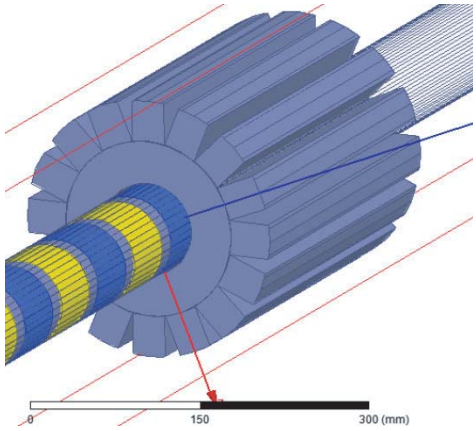

Figure 4. Third stator structure.

perpendicular to the direction of motion (as for the second structure). The number of blocks in this case is greater than the previous configuration in that the surface of the cylinder on which they are distributed is greater and allows to accommodate more of them. The magnetic field lines in this case do not focus immediately inside the blocks as in the previous case. This peculiarity allows the reduction of the magnetic field in the border areas of the blocks, greatly restricting the phenomena of saturation. As regards the eddy currents, the structure allows to confine them always within individual laminations.

The regions of the machine at the interface of the structures with different laminations deserves some discussion. Considering that the lamination of the back iron correctly works when the flux has either axial or radial component, while the lamination of the teeth works when the flux has the radial component only, the laminae constituting the back iron have the shape of combs with short teeth as reported in Figure 5. The disks, which constitute the main portion of the teeth, are assembled and subsequently ground; also, the sectors constituting the back iron are ground in order to minimize the airgap in the regions of contact. Pins are inserted between the back iron and the disks, and spacers are properly introduced between the sectors.

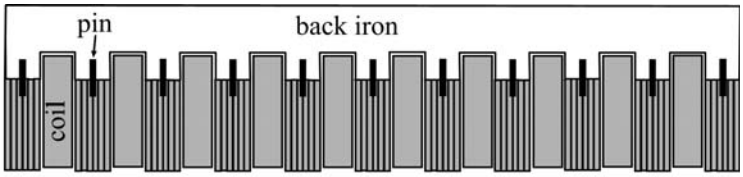

Figure 5. Schematic view of the region at the interface between different laminations.

2.2. Mover Structures

Although in literature there are many examples of linear generators realized with SmCo and NeFeB magnets, in some applications these magnetic materials present some disadvantages. Even thought they give the chance to obtain high values of B*H, they are very expensive [5]. Moreover, NeFeB cannot be used in corrosive environments. The use of ferrite magnets, despite their low values of B*H, enables the work at higher temperatures. Moreover, ferrite magnets are very resistant to corrosion as well as prices rise. As a matter of fact prices for the purchase and maintenance are consistently lower than those of rare earths [6].

Figure 6 shows the translator (or mover). It is composed of ferrite ring magnets and iron rings in almost Halbach configuration. In particular, it is made by stacking four successive magnetic rings axially magnetized and an iron ring. The structure is repeated moving along the axis of the translator. In this way two poles homonyms find themselves facing the same iron ring forcing the lines of flux to branch off radially, across the air gap and reach the stator. The ferrite rings used in the simulations are characterized by $B_r = 0.4\,\mathrm{T}$ and $H_c = 3,178 \cdot 10^5\,\mathrm{A/m}$. The Table 1 contains the geometrical data of the translator.

Table 1. Geometrical data of the translator.

Translator lenght	0.70 m
Number of magnetic rings	36
Internal radius magnetic rings	20 mm
Outside radius magnetic rings	40 mm
Thicknesses magnetic rings	15 mm
Outside radius iron rings	40 mm
Internal radius iron rings	20 mm

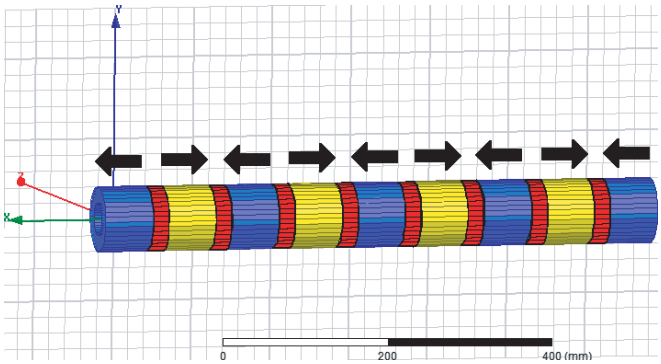

Figure 6. The translator structure.

3. DEVELOPED SIMULATIONS

The three prototypes of machine have been simulated by using a full 3D finite elements model. The machines have been discretized with a large number of elements (200,000 elements for the stator and 100,000 for the mover). The simulations were performed assuming the operation as a generator, being this kind of machines particularly suitable for the conversion of form of mechanical energy of linear type into electrical energy. In particular, the scientific community is nowadays focusing attention on exploring electrical devices able to ensure electrical energy directly from the linear motion of sea waves [7–9].

As an example of mechanical input, starting from an initial position which provides the translator adjacent and completely outside of the stator, a displacement at constant speed of 40 cm/s and with a total duration of one second has been imposed. At its final position the translator has shifted by 40 cm inside the stator. This kind of linear mechanical input is a typical supplying form of sea waves, that we can obtain in Mediterranean sea, both in power and stroke terms. In this case the scientific literature provides several effective solutions for the power electronic converters [10–13]. The stator windings have been connected to a 20 Ω resistive load. In order to assess the effects of the stator structure on the overall performance of the machine, we evaluated the flux linkage with the windings, the induced voltages, the currents, the force along the moving direction and the total iron losses (as the sum of eddy current losses, losses due to magnetic hysteresis and additional losses) [14, 15].

The typology of mechanical input that supplies the generator during the simulation does not allow it to work in steady state conditions. This is a typical working condition for this kind of generators that can be supplied by a discontinuous form of energy like see waves. In this working condition, to evaluate the generator efficiency, we have focused the attention on the quantification of the losses. These three machine topologies have equal mechanical losses as they mount the same mover. Taking into account that the three machines have the same stator resistance, it can be stated that the copper energy loss in each machine, during the simulation, is proportional to the integral of the current square. The values of the copper energy loss calculated for the three machine topologies are the following:

- $E_1 = 0.45\,\mathrm{J}/\Omega$ for the first stator structure;
- $E_2 = 0.45\,\mathrm{J}/\Omega$ for the second stator structure;
- $E_3 = 0.47\,\mathrm{J}/\Omega$ for the third stator structure.

Given the obtained values, it can be therefore stated that the copper losses in the three machines are the same.

If the iron is affected by a sinusoidal flux, iron losses may be calculated in the frequency domain by the following expression

$$P_{Fe} = P_h + P_c + P_a = K_h f B_m^2 + K_c f^2 B_m^2 + K_a f^{1,5} B_m^{1,5} \tag{1}$$

where B_m is the magnetic flux density amplitude, f the frequency, K_h the magnetic hysteresis loss coefficient, K_c the eddy current loss coefficient, and K_a the additional loss coefficient. The coefficient

K_c is calculated by the following expression:

$$K_c = \pi^2 \sigma \frac{d^2}{6} \tag{2}$$

where σ is the material conductivity and d the sheets thickness. The coefficients K_h and K_a are calculated by the sinusoidal flux loss characteristics provided by the manufacturer of sheets at one frequency by varying B_m. In particular, the expression of the overall losses can be rewritten as

$$P_{Fe} = K_1 B_m^2 + K_2 B_m^{1,5} \tag{3}$$

with

$$K_1 = K_h f + K_c f^2 \quad and \quad K_2 = K_a f^{1,5} \tag{4}$$

One proceeds by identifying K_1 and K_2 in such a way as to minimize the function:

$$f(K_1, K_2) = \Sigma [P_{Fei} - (K_1 B_{mi}^2 + K_2 B_{mi}^{1,5})]^2 = \min \tag{5}$$

where P_{Fei} and B_{mi} are respectively the various points of the characteristic of losses provided by the manufacturer. Once K_1 and K_2 have been obtained the other coefficients can be written as:

$$K_h = (K_1 - K_c f_0^2)/f_0 \qquad K_a = K_2/f_0^{1,5} \tag{6}$$

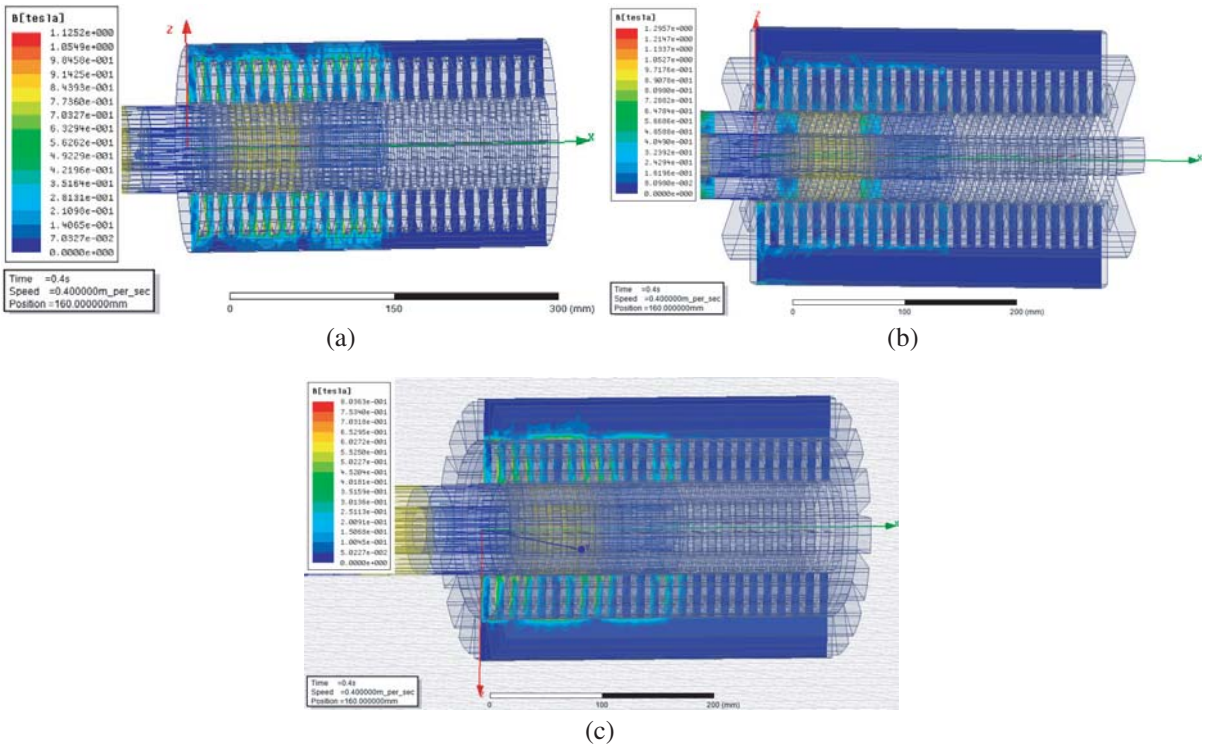

Figure 7. Magnetic flux density in the three different structures. (a) Type 1. (b) Type 2. (c) Type 3.

4. RESULTS

The simulations of the three different structures have allowed to compare the following quantities: flux linkage to triple-wound counterparts, currents passing through triple-wound counterparts, induced voltages in three-winding counterparts, offs and normalized core loss and force along the direction of translation. Figure 7 shows the maps of the magnetic flux density in the three different structures. Figure 8(a) shows the flux linkage diagram with the windings. The data obtained in the simulation are very similar, nevertheless the small differences are to be considered as significant. The figure shows the

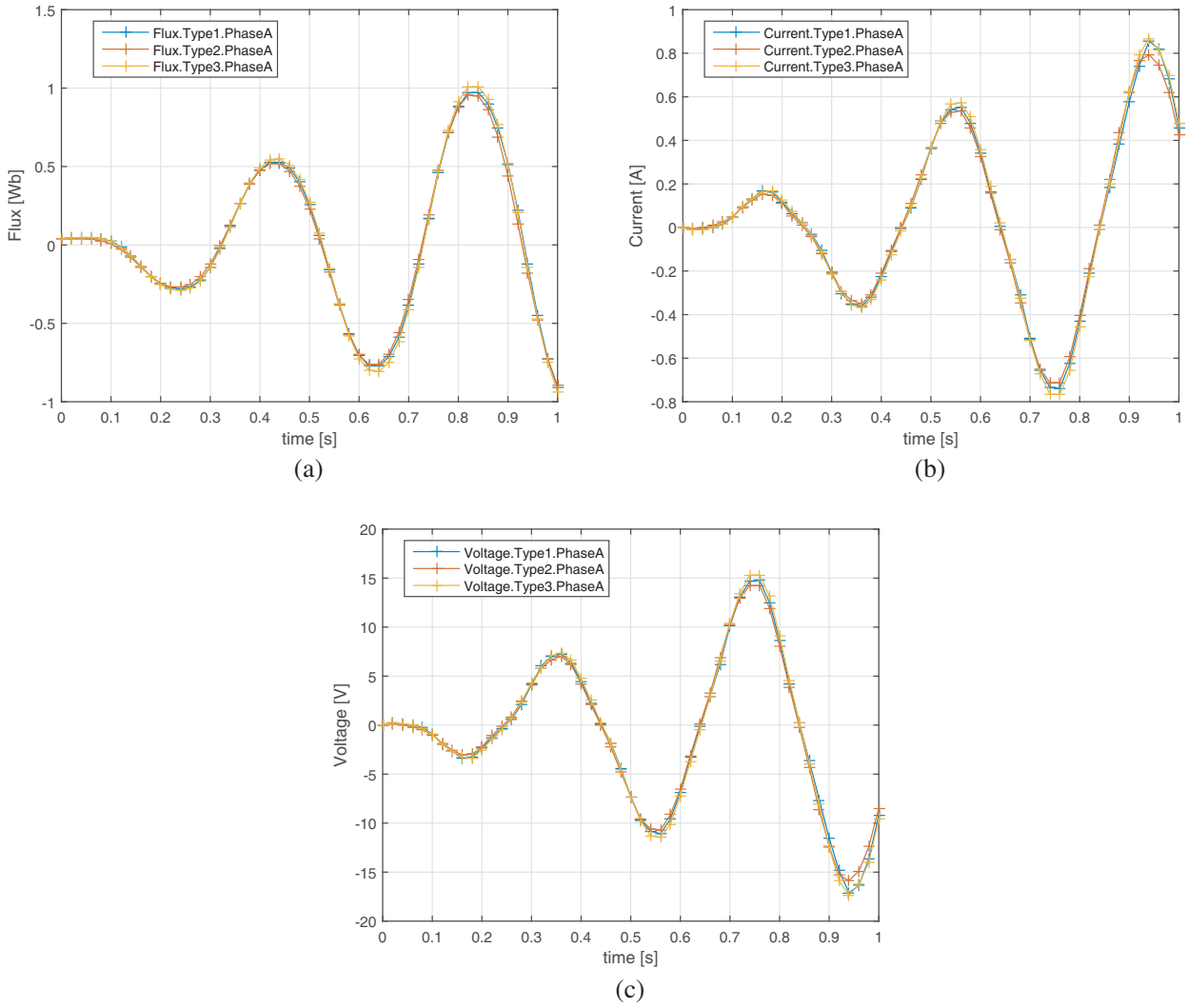

Figure 8. Compared quantities (phase A): Magnetic flux, current and voltage. (a) Flux linkage with phase A. (b) Currents of phase A. (c) Voltage of phase A.

trend of the flux linkage in phase A of the three prototypes. The flux pattern is sinusoidal with amplitude gradually increasing as a function of the translator position inside the stator (initially empty); obviously the time varying voltages (and the currents) induced by the concatenated flux have the same profile. The points obtained are almost superimposable in the first two configurations, while the intensity of the flux is slightly greater for the third type. In fact, in the first structure, the flux is influenced by the presence of the laminations that contribute to increase the air gap. The second lamination does not affect the flux, but the non-homogeneous distribution of flux in the iron around the translator contributes to increase the flux leakage.

In any case, one might conclude that the flux is very similar because the dominant term in the reluctance of the magnetic circuit is given by the air gap. It follows that the two structures are equivalent in terms flux linkage. The third structure, instead, having a lamination perpendicular to the first version, and ensuring a homogeneous distribution of the iron around the translator (unlike the second version), reduces the flux leakage and contributes to the increase of the useful flux. This is also reflected by the performance of stator currents and induced voltages as shown in Figure 8(b) and Figure 8(c) respectively. The analysis shows therefore that the third type of structure contributes to an increase in the overall efficiency of the machine, because for equal structure of the translator and equal movement, the flux linkage, the induced voltages, and then the currents are greater in the third type. Major discrepancies

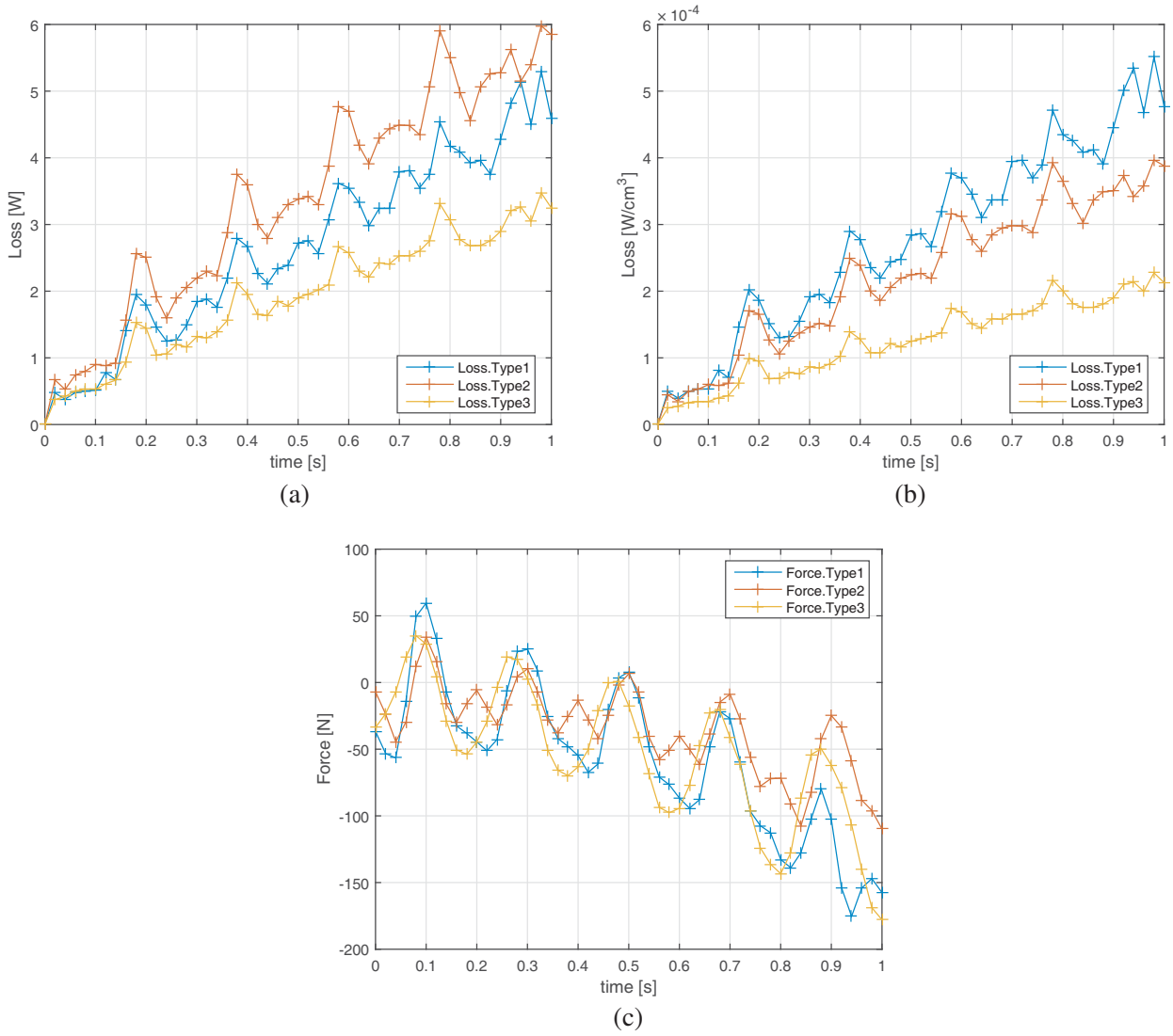

Figure 9. Compared quantities: Iron losses and force. (a) Iron losses. (b) Iron losses narmalized vs. pack size. (c) Force on the mover.

are found instead in the comparison of the iron losses in both absolute terms and in relation to the overall volume. The Figure 9(a) shows total losses in the three structures. The diagram shows that the version of a machine that presents lowest losses is the third, ie the one with innovative hybrid characteristics, while the version of a machine that presents the greatest losses is the second version. However, it is more meaningful to compare the losses normalized to the volume of the machines. Figure 9(b) shows the comparison between the losses of the three structures normalized to the overall dimensions. From the comparison, it is clear that the third version of machine presents the lowest losses. Neglecting the comparison with the first version of the machine, the discrepancy between the second and the third solution should not be affected by the lamination type. In fact both versions allow to confine the currents inside the sheets volume, both for the field in the axial direction and in the radial direction. Then, the difference can be explained considering that due to the more even distribution of the iron around the translator in the third structure, the related eddy currents have lower intensity. Losses are reduced as a consequence.

The third prototype allows us to maintain the lowest value of the magnetic induction because it offers a greater section to the total flux in the part of the teeth that is located near “back iron”. In fact,

this flux has a major impact on flux leakage due to stator currents. It might be useful to take account of the effect of the various structures on the force along the axis of movement. Figure 9(c) shows the trends of the forces in the three structures. Since the translator has a uniform motion, the acceleration is zero. Consequently, the movement direction forces must necessarily balanced. These forces are: the force exerted to get the motion, the resisting electric load force, the end-effect force and the cogging force. Therefore the diagram, unless the resisting electric load force, reports the progress of end-effect force and cogging force. For this type of machine structure (translator long and short stator) and the amount of points earned, we can neglect the cogging force, and therefore trends describe the force due to end-effect. From the comparison of the three diagram, it appears that the machine that presents better characteristics in terms of end-effect is the second, while the worst is the third.

5. CONCLUSIONS

The authors have discussed the comparison of the predicted performance of a PLTLM characterized by three different stator structures, each with its own lamination, while the PM mover remains unchanged. In particular, the machines performances have been evaluated assuming the operation as a generator from sea waves. So a mechanical input, typical to the ones that can be obtained from the waves in Mediterranean sea, has been imposed, and typical shapes of currents and voltages have been obtained. They can be used to load a battery or to produce hydrogen through the interposition of power electronic unit. The analysis of some figures of merit of the three machines, obtained on the basis of accurate 3D FEM based numerical simulations, has allowed us to conclude that the proposed innovative stator configuration, characterized by the presence of two regions with different laminations, is able to improve the performance of the machine by an important reduction of the iron losses.

REFERENCES

1. Di Dio, V. and M. Montana, "State of art of tubular linear induction motor," *8th Mediterranean Electrotechnical Conference, 1996, MELECON '96*, Vol. 1, No. 10, 285–288, 1996.
2. Gieras, J. F., *Linear Induction Drives*, Oxford Univ. Press, New York, USA, 1994.
3. Musolino, A., R. Rizzo, and E. Tripodi, "The double-sided tubular linear induction motor and its possible use in the electromagnetic aircraft launch system," *IEEE Trans. on Plasma Sci.*, Vol. 41, No. 5, 1193–1200, May 2013.
4. Musolino, A., R. Rizzo, and E. Tripodi, "Tubular linear induction machine as a fast actuator: Analysis and design criteria," *Progress In Electromagnetics Research*, Vol. 132, 603–619, 2012.
5. Wang, G., W. Jewell, and D. Howe, "A general framework for the analysis and design of tubular linear permanent magnet machines," *IEEE Trans. Magn.*, Vol. 35, No. 3, 1986–2000, 2010.
6. Cipriani, G., M. Corpora, V. Di Dio, R Miceli, C. Spataro, and M. Trapanese, "Technical and economical comparison between NdFeB and hard ferrites linear electrical generators from sea waves," *International Conference on Renewable Energy Research and Applications (ICRERA)*, 2015.
7. Di Dio, V., G. Cipriani, R. Miceli, and R. Rizzo, "Design criteria of tubular linear induction motors and generators: A prototype realization and its characterization," *Leonardo Electron. J. Practices Technol.*, Vol. 12, No. 23, 23–41, 2013.
8. De O. Falcäo, A. F., "Wave energy utilization: A review of the technologies," *Renewable and Sustainable Energy Reviews*, Vol. 14, No. 3, 899–918, 2010.
9. Cappelli, L., F. Marignetti, G. Mattiazzo, E. Giorcelli, G. Bracco, S. Carbone, and C. Attaianese, "Linear tubular permanent-magnet generators for the inertial sea wave energy converter," *IEEE Transactions on Industry Applications*, Vol. 50, No. 3, 1817–1828, May 2014.
10. Mohamed, K. H., N. C. Sahoo, and T. B. Ibrahim, "A survey of technologies used in wave energy conversion systems," *2011 International Conference on Energy, Automation, and Signal (ICEAS)*, 1–6, Bhubaneswar, Odisha, 2011.

11. Hong, Y., R. Waters, C. Bostrm, M. Eriksson, J. Engstrm, and M. Leijon, "Review on electrical control strategies for wave energy converting systems," *Renewable and Sustainable Energy Reviews*, Vol. 31, 329–342, March 2014, ISSN 1364-0321.
12. Kurupath, V., R. Ekstrm, and M. Leijon, "Optimal constant DC link voltage operation of a wave energy converter," *Energies*, Vol. 6.4, 1993–2006, 2013.
13. Bostrom, C., B. Ekergard, R. Waters, M. Eriksson, and M. Leijon, "Linear generator connected to a resonance-rectifier circuit," *IEEE Journal of Oceanic Engineering*, Vol. 38, No. 2, 255,262, April 2, 2013.
14. Cardelli, E., "A general hysteresis operator for the modeling of vector fields," *IEEE Transactions on Magnetics*, Vol. 47, No. 8, 2056–2067, 2011.
15. Cardelli, A. F. E. and E. Della Torre, "A general vector hysteresis operator: Extension to the 3-d case," *IEEE Transactions on Magnetics*, Vol. 46, 3990–4000, December 2010.